

Manuscript Number: JMBBM-D-16-00321R1

Title: Frequency-modulated atomic force microscopy localises viscoelastic remodelling in the ageing sheep aorta

Article Type: Research Paper

Corresponding Author: Dr. Riaz Akhtar, PhD

Corresponding Author's Institution: University of Liverpool

First Author: Riaz Akhtar, PhD

Order of Authors: Riaz Akhtar, PhD; Helen K Graham; Brian Derby; Michael J Sherratt; Andrew W Trafford; Richard S Chadwick; N ria Gavara

Abstract: Age-related aortic stiffening is associated with cardiovascular diseases such as heart failure. The mechanical functions of the main structural components of the aorta, such as collagen and elastin, are determined in part by their organisation at the micrometer length scale. With age and disease both components undergo aberrant remodelling, hence, there is a need for accurate characterisation of the biomechanical properties at this length scale. In this study we used a frequency-modulated atomic force microscopy (FM-AFM) technique on a model of ageing in female sheep aorta (young: ~18 months, old: >8 years) to measure the micromechanical properties of the medial layer of the ascending aorta. The novelty of our FM-AFM method, operated at 30 kHz, is that it is non-contact and can be performed on a conventional AFM using the 'cantilever tune' mode, with a spatial (areal) resolution of around 1.6  $\mu\text{m}^2$ . We found significant changes in the elastic and viscoelastic properties within the medial lamellar unit (elastic lamellae and adjacent inter-lamellar space) with age. In particular, there was an increase in elastic modulus (Young; geometric mean (geometric SD) = 42.9 (2.26) kPa, Old = 113.9 (2.57) kPa,  $P < 0.0001$ ),  $G'$  and  $G''$  (storage and loss modulus respectively) (Young;  $G' = 14.3$  (2.26) kPa, Old  $G' = 38.0$  (2.57) kPa,  $P < 0.0001$ ; Young;  $G'' = 14.5$  (2.56) kPa, Old  $G'' = 32.8$  (2.52) kPa,  $P < 0.0001$ ). When comparing the lamellar and inter-lamellar regions of the medial layer, the stiffening was found to be more pronounced in the inter-lamellar regions of the vessel. The trends observed in the elastic properties with FM-AFM matched those we have previously found using scanning acoustic microscopy (SAM). The utility of the FM-AFM method is that it does not require custom AFM hardware and can be used to simultaneously determine the elastic and viscoelastic behaviour of a biological sample.

RE: Ms. Ref. No.: JMBBM-D-16-00321

Title: Frequency-modulated atomic force microscopy localises viscoelastic remodelling in the ageing sheep aorta

Dear Professor Simms,

We are grateful to the reviewer for their insightful comments for our draft manuscript. We have amended our paper accordingly. Our responses are in red font below directly after the reviewer's comments.

Reviewer #1: The manuscript "Frequency-modulated atomic force microscopy localises viscoelastic remodelling in the ageing sheep aorta" by R Akhtar et al, attempts to examine the elastic and viscoelastic properties of young and old sheep aorta. The authors argue that the age-related changes in the viscoelastic properties of the tissue are localised to the inter-lamellar regions of the aortic medial layer. They concluded that frequency modulated atomic force microscopy can be used to probe age-related regional variations in the elastic and viscoelastic properties of ovine aorta.

The approach appears interesting and it could lead to useful applications. However, Authors should consider the following issues that could benefit with some further clarification

Major concern

The major problem that I have with this paper are some methodological and conceptual difficulties producing inconsistency in the final results; thus the conclusion sounds unconvincing and is where authors should make an extra effort to justify it.

Statistics analysis: Frequency distributions of the mechanical properties, i.e. elastic modulus (E), storage shear modulus ( $G'$ ) and loss modulus ( $G''$ ), are non Gaussian mainly in young people. It is preferable to use non-parametric central indices like median and mode instead mean values. Even more, it's not proper the use of the standard error (SE) instead of the standard deviation (SD), since it is a measure of how far the sample mean is likely to be from the true population mean.

We have performed normality tests to verify whether the data followed a normal or log-normal distribution (which would then inform the use of means or geometric means as suitable descriptors of the distribution). Our tests indicate that data from both old and young samples is log-normally distributed. Accordingly, we have replaced the values presented in table 1 and throughout the manuscript, to be presented as geometric mean (geometric standard deviation).

What do Authors mean with the sentence stating "Both  $G'$  and  $G''$  increased with age in the lamellar and inter-lamellar regions but the most statistically significant P-values were found in the interlamellar regions" in line 50, page 9?

We have changed this confusing sentence to ‘Both  $G'$  and  $G''$  increased with age in the lamellar and inter-lamellar regions’.

In this reviewer’s opinion average values are close similar. Is it a variance issue? Do Authors perform a repeatability and reproducibility study?

Please improve the statistical analysis section. It could be useful for the average reader.

In terms of repeatability and reproducibility, as stated in Section 2.2, we selected 11 random locations on 3 individual tissue sections for each sample. We have already tested the feasibility of the technique and its reproducibility on tissues and model materials (gels) in our previously published work (Gavara and Chadwick, 2010). We have added to the manuscript a short analysis of the variability of the results by performing coefficient of variance (CoV) analysis of our data. Typically, a homogeneous material will display similar CoV values when analyzing inter- and intra-sample variability. Interestingly, we find that intra-tissue variability is larger than inter-animal variability in our data. This finding reinforces the notion that the medial layer is heterogeneous (lamellar and inter-lamellar regions have different mechanical properties). Furthermore, the finding that CoV is smaller for inter-animal comparisons suggests we have probed a large enough number of tissue locations to obtain a reliable estimate for the overall mechanical properties for each animal.

We thank the reviewer for pointing out the limitations in our statistical analysis section. This has now been substantially improved in the revised manuscript.

Mechanical properties: The text is rather patchy and not clear at times, for instance the calculation of mechanical parameters is scarcely explanatory. Authors wrote The elastic modulus (E), storage shear modulus ( $G'$ ), loss modulus ( $G''$ ) and loss tangent ( $G''/G'$ ) were determined using the formulas reported previously [16]”. Cite [16] does not exist; neither the calculation of the loss tangent. Please include loss tangent values as well as the analysis of this property in the Discussion section.

- We apologize for this error. We changed from numbered to Harvard referencing as per the requirements of the journal and erroneously left an old citation in the manuscript. This reference referred to our Nature Methods paper (Gavara and Chadwick, 2010). We have taken on board the concern of the reviewer and substantially expanded this section. The updated text in Section 2.3 is as follows:
- *The theory to estimate elastic modulus (E) and effective viscosity ( $\mu_{eff}$ ), using the changes in frequency and phase of cantilever oscillation has been developed elsewhere (Gavara and Chadwick, 2010). . The formulas used are:*

$$- E = \left(\frac{9k\Delta f}{c_0}\right)^{3/2} \rho^{-1/2} a_0^{-2} (2\pi f_\infty)^{-5/2} \left(1 - \frac{6}{f} \frac{df}{d\phi}\right)^{-1} \left(h_{200}^{1/3} - h_{50}^{1/3}\right)^{-3/2} \quad [1]$$

$$- \mu_{eff} = \frac{3E \frac{df}{d\phi}}{\pi f^2} \quad [2]$$

- where  $c_0 = 0.3419$ ;  $k$  is the stiffness of the cantilever,  $\Delta f$  is the frequency shift (Hz) where the phase is  $\pi/2$ ;  $\rho$  is the density of water,  $a_0$  is the radius of the bead attached to the end of the cantilever,  $f$  is the frequency where the phase is  $\pi/2$ ;  $f_\infty$  is the frequency far from the sample;  $d\phi/df$  is the slope of the phase-frequency curve where the phase is  $\pi/2$ .

- We can then obtain further viscoelastic parameters such as storage shear modulus ( $G'$ ), loss modulus ( $G''$ ) and loss tangent ( $G''/G'$ ) as follows:

$$G' = \frac{E}{2(1+\nu)} \quad [3]$$

$$G'' = 2\pi f \mu_{eff} \quad [4]$$

- where  $\nu$  is the Poisson's ratio of the sample and it is assumed to be 0.5.
- We have now added loss tangent results to the end of Section 3.1 and a sentence to the Discussion. The text is reproduced below:
- *The loss tangent was lower in the old group as compared to the young group (young = 1.0 (1.94); old = 0.86 (1.2)) but the difference was not significant (P=0.28). Finally, when comparing the intra-tissue versus inter-animal variability of our data, we found that the CoV (coefficient of variance) was largest for data obtained at different locations of the same tissue, rather than the CoV arising from data from different animals (intra-tissue CoV =  $26.5 \pm 16.7$  (mean  $\pm$  SD); inter-animal CoV =  $16.6 \pm 7.7$  (mean  $\pm$  SD) but the difference was not significant (P=0.09).*

- In the discussion we have added:
- *With age  $G'$  and  $G''$  increased by the same relative amount as determined by the loss tangent data.*

- Others concerns:

An additional area that requires clarification is about the values of E and  $G'$ . The difference with the absolute elastic value of elastin fibers deserves deeper explanations.

Our results for E correspond to the stiffness displayed by networks mainly composed of elastic and collagen fibres, rather than the absolute elastic value of elastin or collagen. It is worth mentioning that the stiffness of a polymeric network will depend not only on the elastic modulus of the fibres composing it, but also on their density and the presence (or not) of cross-linking elements. Finally, being typically low-density sparsely-crosslinked, biopolymeric networks tend to display stiffness much lower than those reported for the constituent fibres. We have added a couple of sentences to the manuscript to clarify this issue, and citations to our previous work comparing stiffness values for networks vs individual fibres.

What is the anatomical correlate of  $G''$  modulus? It could be close to the viscous behavior of smooth muscle fibers.

*G'' is likely to be mainly influenced by the smooth muscle component of the vessel wall as the reviewer states. We mentioned this in our discussion with a supporting reference on page 13: 'Furthermore, as summarised by Holzapfel et al. (Holzapfel et al., 2002), numerous studies have reported that smooth muscle cells are primarily responsible for the viscoelastic behaviour of arteries.'*

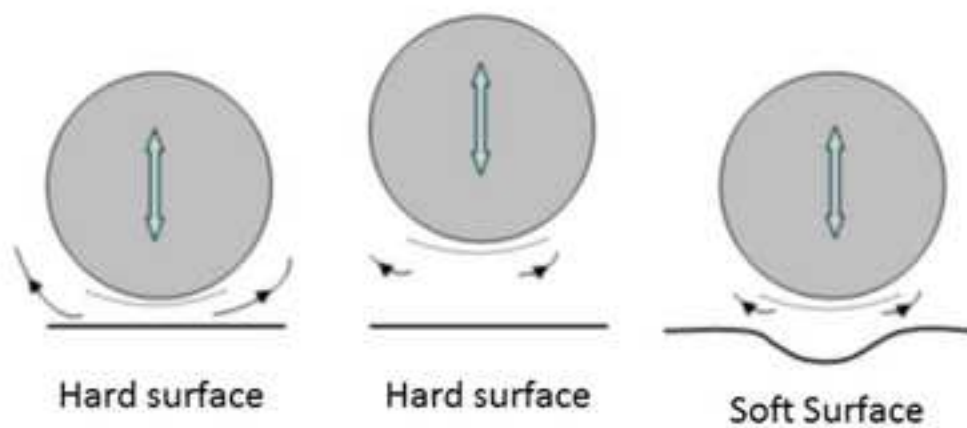
On this point, I am confused: Why do Authors use in the abstract different values from table 1?

*We apologise for this error. This has now been corrected. The same values appear in the Abstract as Table 1.*

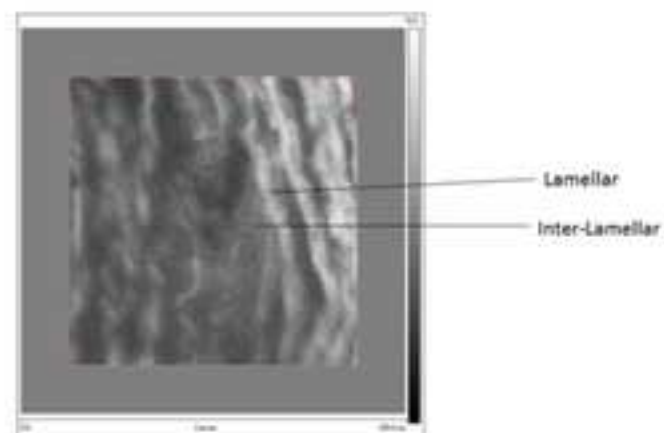
Figures 2 and 3 including 11 panels seem a little too much. It should be revised and reduced

*We disagree with the reviewer on this point and feel that two separate panel figures of 4 and 6 graphs are a suitable way of presenting the data and showing the trends obtained. These are in line with other papers in this journal.*

### Frequency-modulated atomic force microscopy



### Aortic medial layer characterisation



**Frequency-modulated atomic force microscopy localises viscoelastic remodelling in the ageing  
sheep aorta**

R Akhtar<sup>1</sup>, H.K. Graham<sup>2</sup>, B Derby<sup>3</sup>, MJ Sherratt<sup>2</sup>, A.W. Trafford<sup>4</sup>, R.S. Chadwick<sup>5</sup>, N. Gavara<sup>6</sup>

<sup>1</sup> Centre for Materials and Structures, School of Engineering, University of Liverpool, L69 3GH.

<sup>2</sup> Institute of Inflammation and Repair, Manchester Academic and Health Sciences Centre, Stopford Building, The University of Manchester, Oxford Road, Manchester M13 9PT, UK.

<sup>3</sup> School of Materials, The University of Manchester, Oxford Road, Manchester, M13 9PL.

<sup>4</sup> Institute of Cardiovascular Sciences, Faculty of Medical and Human Sciences, The University of Manchester, 46 Grafton Street, Manchester, M13 9NT.

<sup>5</sup> Auditory Mechanics Section, National Institute on Deafness and Other Communication Disorders, National Institutes of Health, Bethesda, Maryland, USA.

<sup>6</sup> School of Engineering and Materials Science, Queen Mary University of London, Mile End Road, London, E1 4NS, UK.

Corresponding Author: Dr Riaz Akhtar, Centre for Materials and Structures, School of Engineering, University of Liverpool, L69 3GH, United Kingdom.

Tel. +44151 794 5770, Fax +44161 794 4703, Email: [r.akhtar@liverpool.ac.uk](mailto:r.akhtar@liverpool.ac.uk)

**Conflict of interest statement**

*There are no conflicts of interest to declare.*

1  
2  
3 **Abstract**  
4  
5  
6  
7

8 Age-related aortic stiffening is associated with cardiovascular diseases such as heart failure.  
9  
10 The mechanical functions of the main structural components of the aorta, such as collagen  
11 and elastin, are determined in part by their organisation at the micrometer length scale. With  
12 age and disease both components undergo aberrant remodelling, hence, there is a need for  
13 accurate characterisation of the biomechanical properties at this length scale. In this study we  
14 used a frequency-modulated atomic force microscopy (FM-AFM) technique on a model of  
15 ageing in female sheep aorta (young: ~18 months, old: >8 years) to measure the  
16 micromechanical properties of the medial layer of the ascending aorta. The novelty of our  
17 FM-AFM method, operated at 30 kHz, is that it is non-contact and can be performed on a  
18 conventional AFM using the ‘cantilever tune’ mode, with a spatial (areal) resolution of  
19 around  $1.6 \mu\text{m}^2$ . We found significant changes in the elastic and viscoelastic properties within  
20 the medial lamellar unit (elastic lamellae and adjacent inter-lamellar space) with age. In  
21 particular, there was an increase in elastic modulus (Young; geometric mean (geometric SD)  
22 = 42.9 (2.26) kPa, Old = 113.9 (2.57) kPa,  $P < 0.0001$ ),  $G'$  and  $G''$  (storage and loss modulus  
23 respectively) (Young;  $G' = 14.3$  (2.26) kPa, Old  $G' = 38.0$  (2.57) kPa,  $P < 0.0001$ ; Young;  $G''$   
24 = 14.5 (2.56) kPa, Old  $G'' = 32.8$  (2.52) kPa,  $P < 0.0001$ ). When comparing the lamellar and  
25 inter-lamellar regions of the medial layer, the stiffening was found to be more pronounced in  
26 the inter-lamellar regions of the vessel. The trends observed in the elastic properties with FM-  
27 AFM matched those we have previously found using scanning acoustic microscopy (SAM).  
28 The utility of the FM-AFM method is that it does not require custom AFM hardware and can  
29 be used to simultaneously determine the elastic and viscoelastic behaviour of a biological  
30 sample.  
31  
32  
33  
34  
35  
36  
37  
38  
39  
40  
41  
42  
43  
44  
45  
46  
47  
48  
49  
50  
51  
52  
53  
54  
55  
56  
57  
58  
59  
60  
61  
62  
63  
64  
65



## 1. Introduction

Ageing is associated with arterial stiffening and the development of cardiovascular disease. Stiffening in large arteries such as the aorta is typically studied at the level of the whole vessel. However, there is now evidence which suggests that alterations in the structure and mechanical properties of large arteries at the micron scale can have detrimental effects on the function of the aorta (Kohn et al., 2015). Hence, there is growing interest in characterizing the nano- and micro-mechanical properties of the aorta to better understand the structure-property-function relationships within large arteries (Akhtar et al., 2014; Akhtar et al., 2009; Grant and Twigg, 2013; Kohn et al., 2015). Due to the intricate organisation of extracellular matrix (ECM) components within the vessel wall, there is a need to develop methods that accurately measure the mechanical properties of the tissue with high spatial resolution. However, due to a lack of appropriate techniques, there is still limited information on these properties at the micron length scale (Graham et al., 2011). Accessing this information is vital because both force-sensing cells and large ECM assemblies such as collagen and elastic fibres, which govern the mechanical response of large arteries, are organised at this length scale (Akhtar et al., 2011). Hence, there is a need to develop reliable, quantitative methods for the assessment of the mechanical properties of vascular tissue at the micron length scale (Akhtar, 2014; Akhtar et al., 2009).

Our previous work focussed on the use of scanning acoustic microscopy (SAM) to determine regional variations in the elastic properties of the aorta at this length scale (Akhtar et al., 2014; Graham et al., 2011; Lopez-Andres et al., 2012). SAM measures the speed of longitudinal acoustic waves through a material, which can be related to its elastic modulus. When SAM is operated at frequencies close to 1 GHz, it provides quantitative measurements of acoustic wave speed with a linear spatial resolution around 1  $\mu\text{m}$ . Using this technique we have shown that changes in the micromechanical properties of the aorta that occur with age and with pathology (diabetes), can be localised to the inter-lamellar regions of the medial lamellar unit (MLU) within the aorta. The MLU is the main load-bearing component of the aortic wall and is composed of an elastin-rich lamellae and a fibrillar collagen with a vascular smooth muscle cell-rich inter-lamellar region (O'Connell et al., 2008).

Although the use of SAM for measuring the properties of soft tissues such as the aorta has a number of advantages, including co-localisation of histological and elastic properties and fast data acquisition (Zhao et al., 2012), SAM cannot provide information on the viscoelastic and

1 time-dependant response of tissue, because it operates at low amplitude acoustic deformation  
2 rates, and is limited to characterising tissue stiffness indirectly because acoustic wave speed  
3 is a function of both elastic modulus and local density. Another technique for acquiring  
4 mechanical properties is a contact or indentation method such as atomic force microscopy  
5 (AFM) which can be used to measure the elastic and viscoelastic properties of tissues at a  
6 higher spatial resolution than SAM, and has been used, for example, to characterise intimal  
7 stiffening in the aorta (Huynh et al., 2011).  
8  
9  
10  
11

12  
13 Despite the relatively wide use of AFM for biological applications, AFM-indentation  
14 approaches are not always ideal for probing soft biological tissues due to lengthy acquisition  
15 times and also the requirement of the probe to be either continuously or intermittently in  
16 contact with the sample. A comparison of acoustic and AFM methods for the characterisation  
17 of tissue has been reviewed elsewhere (Akhtar et al., 2011)..  
18  
19  
20  
21  
22

23 Frequency-modulated atomic force microscopy (FM-AFM) is an AFM mode which  
24 overcomes some of these issues and can be employed by existing commercial AFM systems.  
25 The principle of FM-AFM is that it relies on detecting small changes in the cantilever  
26 resonant frequency, which occur in response to the tip-sample interaction (Higgins et al.,  
27 2005). These frequency shifts can then be used to measure force interactions between the tip  
28 and sample. Although there are concerns about uncertainty when AFM techniques are used  
29 for mechanical property characterisation e.g. due to complications arising due to tip-sample  
30 interactions (Lin et al., 2009), AFM methods are nevertheless powerful tools for the nano-  
31 and micro-scale characterisation of soft tissues. When probing the difference between two  
32 samples, any uncertainty can be minimised by utilising the same tip and configuration to  
33 provide more robust mechanical property data.  
34  
35  
36  
37  
38  
39  
40  
41  
42  
43

44 FM-AFM is a powerful tool for studying the mechanical properties of single biomolecular  
45 interactions and force-extension response of isolated molecules in liquid (Higgins et al.,  
46 2005; Humphris et al., 2000). FM-AFM has previously been applied to biological systems to  
47 study single polysaccharide molecules (Humphris et al., 2000) and DNA (Cerreta et al.,  
48 2013), for example. Gavara and Chadwick developed the technique further, specifically for  
49 applications in the study of the microrheology of biological tissues that produce or detect  
50 sound (Gavara and Chadwick, 2010). In that work, they demonstrated that material properties  
51 of gels and soft biological tissue can be determined via frequency modulation based on  
52 hydrodynamics theory of thin gaps that they developed. The key advantages of this method  
53  
54  
55  
56  
57  
58  
59  
60  
61  
62

1 are that it overcomes the limitations of contact and tapping-mode AFM because the probe  
2 does not make any direct contact with the sample (Gavara and Chadwick, 2010). Further, the  
3 amount of force applied onto the sample is reduced to the scale of  $10^{-12}$  N (piconewtons, pN).  
4 The technique was validated by characterising polyacrylamide gels of different stiffness, as  
5 well as determining regional variations in the elastic and viscoelastic properties of soft  
6 biological tissue in near-physiological conditions.  
7  
8  
9

10  
11 In this paper, we apply the FM-AFM method to examine the elastic and viscoelastic  
12 properties of young and old sheep aorta. We show that age-related changes in the viscoelastic  
13 properties of the tissue are localised to the inter-lamellar regions of the aortic medial layer.  
14  
15  
16  
17

## 18 **Material and methods**

### 19 **2.1 Tissue samples**

20  
21 Testing was conducted on ascending aortae from young (~1.5 years, n=5) and old (>8 years,  
22 n=5) female sheep (*Ovis aries*). Sheep were killed by intravenous injection of  
23 pentobarbitone (200 mg/kg) (Dibb et al., 2004) and the ascending aorta rapidly removed.  
24 The aorta was then frozen in optimal cutting temperature (OCT) compound (Sakura Finetek  
25 Europe B.V., The Netherlands) and transverse cryosections were subsequently taken with 5  
26  $\mu\text{m}$  thickness and adsorbed onto glass slides. The sections were kept frozen at  $-80^{\circ}\text{C}$  before  
27 being thawed and hydrated in Phosphate Buffered Saline (PBS) for mechanical testing.  
28  
29  
30  
31  
32  
33  
34  
35  
36  
37  
38  
39  
40  
41

### 42 **2.2 Frequency-Modulated Atomic Force Microscopy**

43  
44 Measurements were performed using a Bioscope Catalyst AFM instrument (Bruker, Billerica,  
45 MA, USA) mounted on the stage of an Axiovert 200 inverted microscope (Carl Zeiss,  
46 Göttingen, Germany) placed on a vibration-isolation table (Newport Isostation, Irvine, CA,  
47 USA). A 10  $\mu\text{m}$  diameter latex bead glued to a tipless V-shaped gold-coated silicon nitride  
48 cantilever (Veeco NP-020, Bruker, Billerica, MA, USA) was used as a probe. The spring  
49 constant of the cantilever was  $0.1942\text{ N m}^{-1}$ . As described in detail by Gavara and Chadwick  
50 (Gavara and Chadwick, 2010), FM-AFM was carried out using the 'cantilever tune' feature of  
51 the tapping mode to sweep the cantilever drive frequency over a selectable frequency range.  
52 A key feature of the cantilever tune mode is the ability to perform frequency sweeps at a  
53  
54  
55  
56  
57  
58  
59  
60  
61  
62  
63  
64  
65

1 controlled height over the sample's surface with nanometre resolution (in the z-direction).  
2 Extensive details of the methodology and underlying theory are reported elsewhere (Gavara  
3 and Chadwick, 2010).  
4  
5

6 All measurements were performed with the tissue sections hydrated in PBS solution at room  
7 temperature. For each test, the cantilever tune mode was utilised to position the tip of the  
8 cantilever 200 nm above the sample. An initial frequency sweep was performed to locate  $f_{\pi/2}$   
9 of interest, that is, the frequency at which we observed a  $\pi/2$  phase difference between the  
10 oscillation of the piezo and the cantilever. In addition, the drive amplitude of the piezo was  
11 adjusted to ensure that the amplitude of oscillation of the cantilever at  $f_{\pi/2}$  was below 5 nm.  
12 Frequency sweeps were recorded with a 3 kHz frequency range around  $f_{\pi/2}$ . Sweeps were  
13 performed for two distances between the bead and the sample, 50 nm and 200 nm. For each  
14 bead-sample distance, five sweeps were recorded in order to reduce inherent variability  
15 associated with AFM measurements. Thus, 10 frequency sweeps were used to calculate the  
16 mechanical properties for a given location i.e. each individual measurement was determined  
17 from 2 tip-sample distances, which were in turn averaged from 5 measurements at each of  
18 these distances (as outlined below in 2.3).  
19  
20  
21  
22  
23  
24  
25  
26  
27  
28  
29  
30

31 To determine the overall properties of the medial layer of the aortic wall, 11 random locations  
32 were selected on 3 tissue sections for each animal. In addition, the fluorescence microscope  
33 incorporated within the AFM system was used to identify and locate lamellar and inter-  
34 lamellar regions of the tissue using elastin auto- fluorescence (**Error! Reference source not  
35 found.**) and 5 lamellar and 5 inter-lamellar locations were selected on 3 tissue sections for  
36 each animal.  
37  
38  
39  
40  
41  
42  
43  
44  
45  
46

### 47 **2.3 Data processing**

48  
49 All data were processed using Matlab (Mathworks, Natick, MA, USA). For each recorded  
50 frequency sweep, phase-frequency curves were fitted with a second-order polynomial around  
51 the  $\pi/2$  to determine  $f_{\pi/2}$ . Values of  $f_{\pi/2}$  for the five frequency sweeps recorded at each height  
52 were used to determine a mean value. **The theory to estimate elastic modulus (E) and  
53 effective viscosity ( $\mu_{\text{eff}}$ ), using the changes in frequency and phase of cantilever oscillation  
54 has been developed elsewhere (Gavara and Chadwick, 2010). . The formulas used are:**  
55  
56  
57  
58  
59  
60  
61  
62  
63  
64  
65

$$E = \left(\frac{9k\Delta f}{c_0}\right)^{3/2} \rho^{-1/2} a_0^{-2} (2\pi f_\infty)^{-5/2} \left(1 - \frac{6}{f} \frac{df}{d\phi}\right)^{-1} \left(h_{200}^{1/3} - h_{50}^{1/3}\right)^{-3/2} \quad [1]$$

$$\mu_{eff} = \frac{3E \frac{df}{d\phi}}{\pi f^2} \quad [2]$$

where  $c_0 = 0.3419$ ;  $k$  is the stiffness of the cantilever,  $\Delta f$  is the frequency shift (Hz) where the phase is  $\pi/2$ ;  $\rho$  is the density of water,  $a_0$  is the radius of the bead attached to the end of the cantilever,  $f$  is the frequency where the phase is  $\pi/2$ ;  $f_\infty$  is the frequency far from the sample;  $d\phi/df$  is the slope of the phase-frequency curve where the phase is  $\pi/2$ .

We can then obtain further viscoelastic parameters such as storage shear modulus ( $G'$ ), loss modulus ( $G''$ ) and loss tangent ( $G''/G'$ ) as follows:

$$G' = \frac{E}{2(1+\nu)} \quad [3]$$

$$G'' = 2\pi f \mu_{eff} \quad [4]$$

where  $\nu$  is the Poisson's ratio of the sample and it is assumed to be 0.5.

The frequency shift used in these calculations was the mean value across 3 different tissue sections for each animal.

## 2.4 Statistical Analysis

We carried out normality tests on the data distributions obtained, as well as on the logarithm of the data distributions. The results of the normality test indicate that the majority of the data obtained followed a log-normal distribution. Accordingly, results are expressed as geometric mean and geometric standard deviation, geomean (geoSD). Statistical analysis has been conducted with the non-parametric Mann-Whitney and Kruskal-Wallis ANOVA tests.

## 3. Results

### 3.1. Mechanical remodelling in the medial layer

The variation in mechanical properties between individual animals is shown in Figure 2a. With the exception of one individual sample, the mean and median values were higher in the old group as compared to the young group. All of the remaining data are presented comparing

1 overall trends in the young vs old group. E, G' and G'' were all significantly higher in the old  
2 group as compared with the young group (Table 1). The frequency distributions (young vs  
3 old) were relatively similar for E, G' and G'' (Figures 2b-2d).  
4  
5  
6  
7  
8  
9

10  
11 The loss tangent was lower in the old group as compared to the young group (young = 1.0  
12 (1.94); old = 0.86 (1.2)) but the difference was not significant (P=0.28). Finally, when  
13 comparing the intra-tissue versus inter-animal variability of our data, we found that the CoV  
14 (coefficient of variance) was largest for data obtained at different locations of the same tissue,  
15 rather than the CoV arising from data from different animals (intra-tissue CoV =  $26.5 \pm 16.7$   
16 (mean  $\pm$  SD); inter-animal CoV =  $16.6 \pm 7.7$  (mean  $\pm$  SD) but the difference was not  
17 significant (P=0.09).  
18  
19  
20  
21  
22  
23

### 24 25 **3.2. Localised mechanical properties of lamellar and inter-lamellar regions**

26  
27 The elastic modulus frequency distributions were profoundly different in the lamellar and  
28 inter-lamellar regions of the media, as shown in Figure 3. The mean data are summarised in  
29 Table 2. The elastic modulus was significantly higher in the old group for both the lamellar  
30 and inter-lamellar regions of the medial layer. Both G' and G'' increased with age in the  
31 lamellar and inter-lamellar regions.  
32  
33  
34  
35  
36  
37  
38  
39  
40  
41  
42

### 43 **4. Discussion**

44  
45 The FM-AFM technique is shown to be a powerful tool for quantitatively assessing regional  
46 differences in the mechanical properties of soft tissues such as the aorta. As applied in this  
47 study, it has provided new insights into the age-related viscoelastic behaviour of the ovine  
48 aorta. This is the first study, to the best of our knowledge, to show how both the elastic and  
49 viscoelastic properties vary within the medial lamellar unit with age. FM-AFM overcomes  
50 the various issues of contact or intermittent contact mode AFM when used for mechanical  
51 measurements, such as using the appropriate contact mechanics model for accounting for tip-  
52 sample interaction (Lin et al., 2009). The main advantage of this technique is that it is a non-  
53  
54  
55  
56  
57  
58  
59  
60  
61  
62  
63  
64  
65

1 contact method, which means that much lower forces and hence local deformations are  
2 applied to soft, biological tissues than with other AFM-based indentation techniques (Gavara  
3 and Chadwick, 2010). Given that experiments in this study were conducted on thin  
4 cryosections of tissue, it seems that the low force applied with this non-contact avoids the  
5 overestimation of the mechanical properties of the tissue due to the glass substrate, which is a  
6 typical challenge with AFM and nanoindentation techniques [6].  
7  
8  
9

10  
11 Additionally, a significant advantage of the FM-AFM method is that no hardware  
12 modifications are required in order to oscillate the cantilever tip at kilohertz frequencies and  
13 nanometer-scale amplitudes, whilst simultaneously controlling the distance between the  
14 probe and the sample surface. Simply, the ‘cantilever tune’ mode of the Bioscope II AFM  
15 instrument can be used. The advantage of using AFM for indentation over nanoindentation is  
16 that a higher spatial resolution is obtained and AFM techniques are considered better suited to  
17 measuring the properties of extremely compliant materials (Akhtar et al., 2011).  
18  
19  
20  
21  
22  
23  
24

25 The mean values for elastic modulus determined in this study lie within the range that has  
26 been reported in the literature for the aorta using indentation-based techniques but on full  
27 thickness sections of tissue (Hemmasizadeh et al., 2012; Matsumoto et al., 2004), (McKee et  
28 al., 2011). McKee et al. reviewed and collated data from a number of studies on vascular  
29 tissues and reported an average value of approximately 125 kPa. None of these studies  
30 compare age-related changes in the aortic wall but provide suitable data for comparison with  
31 our work. The study by Matsumoto et al. focussed solely on characterising the MLU in  
32 porcine aorta (2-3 mm thick specimens) with a micro-indentation device reported a range of  
33 50-180 kPa (Matsumoto et al., 2004), which also fits in with the range in our study.  
34 Hemmasizadeh et al. (Hemmasizadeh et al., 2012) used a nanoindentation technique on full  
35 thickness specimens and reported data for the ‘outer’ (adventitia) and inner (‘media’) layers  
36 of the porcine thoracic aorta. Their elastic modulus measurements corresponding to the  
37 medial layer were around 60 kPa. Here, we demonstrate that we are able to obtain values  
38 within this range on thin cryosections of tissue (5  $\mu\text{m}$ ) hence confirming that the low force  
39 applied with FM-AFM does not lead to a significant substrate effect.  
40  
41  
42  
43  
44  
45  
46  
47  
48  
49  
50  
51  
52

53 Both the  $G'$  and  $G''$  followed the same trends as observed with the elastic modulus data.  
54 However, the trends in the data are dominated by the elastic properties of the aortic wall ( $G'$ ).  
55 Both of these parameters increased with age, as has been reported with dynamic mechanical  
56 measurement techniques e.g. (Yin et al., 1983). **With age  $G'$  and  $G''$  increased by the same**  
57  
58  
59  
60  
61  
62  
63  
64  
65

1 relative amount as determined by the loss tangent data. Furthermore, the increase of  $G'$  and  $G''$   
2 with age was observed in both the lamellar and inter-lamellar regions of the vessel. Age-  
3 related arterial degradation is associated with fatigue failure of elastin and associated  
4 stiffening of the vessel (Greenwald, 2007) and a decline in viscoelastic properties (Yin et al.,  
5 1983). Our data suggests that the largest alterations to the viscoelastic properties of the aorta  
6 with age is largely localised to the inter-lamellar regions. This is not surprising given that the  
7 inter-lamellar region is an intricate meshwork of collagen fibres, elastin-fibres and smooth  
8 muscle cells, and changes in the interface between these components during ageing are  
9 thought to lead to changes in the viscoelasticity of the vessel wall (Silver et al., 2001). It is  
10 worth stressing that the measurements performed here establish the mechanical properties of  
11 elastin and collagen-rich hydrogel matrices, rather than the material properties of collagen or  
12 elastic fibres. Accordingly, we have previously reported that *in vitro*-generated collagen-  
13 based hydrogels or collagen-rich fibroblast-generated matrices display elastic modulus values  
14 much lower (Gavara et al., 2008; Petrie et al., 2012) than native collagen fibres (Gosline et  
15 al., 2002). Furthermore, as summarised by Holzapfel et al. (Holzapfel et al., 2002), numerous  
16 studies have reported that smooth muscle cells are primarily responsible for the viscoelastic  
17 behaviour of arteries.

18  
19  
20  
21  
22  
23  
24  
25  
26  
27  
28  
29  
30  
31  
32 The overall trends in the elastic properties that we found in the FM-AFM data are consistent  
33 with those we have reported previously using ultra-high frequency SAM (Graham et al.,  
34 2011), i.e. stiffening is largely localised to the inter-lamellar regions of the aortic wall. In the  
35 lamellar regions, 8 % of the elastic modulus values were greater than 100 kPa in the young  
36 group as compared to 38 % in the old group. In contrast, in the inter-lamellar regions, 8 % of  
37 the elastic modulus values were greater than 100 kPa as compared to 50 % in the old group.  
38 This large shift in the elastic modulus within the inter-lamellar regions fits with the  
39 histological observations that we reported previously (Graham et al., 2011), and well-  
40 established alterations that occur in the main structural components of the aorta with age,  
41 namely elastin and collagen (Greenwald, 2007). However, there are a number of differences  
42 between the two techniques which are summarised here. The FM-AFM method was  
43 conducted around 30 kHz whereas the SAM work was conducted around 1 GHz (Graham et  
44 al., 2011). The linear spatial resolution of SAM is determined by the operating frequency  
45 (around 1  $\mu\text{m}$ ) in our previous study. With FM-AFM, the spatial resolution is determined by  
46 the size of the probe. Although a 10  $\mu\text{m}$  bead was used in this study with the the FM-AFM  
47 setup, the estimated contact area is 1.6  $\mu\text{m}^2$ . As described by Gavara and Chadwick (Gavara  
48  
49  
50  
51  
52  
53  
54  
55  
56  
57  
58  
59  
60  
61  
62  
63  
64  
65



and Chadwick, 2010), the tip radius and also the bead-sample gap determine the contact area. Thus, the effective areal spatial resolution is much lower than the 10  $\mu\text{m}$  bead utilised in the study. SAM only provides a measure of the acoustic wave speed which is related to the elastic modulus of the tissue. The FM-AFM technique also provides a measure of the storage modulus and loss modulus, although at 30 kHz in the current setup. This is because the largest resonant peak displayed by the cantilever was used as the probing frequency. It is possible to conduct experiments at other frequencies by selecting cantilevers with a different shape or stiffness (Gavara and Chadwick, 2010). Crucially, compared with SAM, the FM-AFM was more sensitive to mechanical remodelling in the elastic lamellae. This may be related to the way in which the measurements have been carried out with SAM as with this approach images were, in some instances, difficult to interpret. Accordingly, only the central-third of pixels were analysed for the lamellar and inter-lamellar measurements. For the FM-AFM technique, accurate placement of the probe over the lamellar or inter-lamellar region was limited to the optical resolution of the associated epifluorescence microscope (Figure 1). Finally, as stated earlier, SAM is a highly specialised technique whereas AFM is a much more accessible technique for many research groups. Hence, the FM-AFM method used in this study has an additional advantage in that it can be readily adopted using conventional AFM instruments. The FM-AFM method could therefore be used for a wide range of applications related to biological sample characterisation.

Future work on vascular tissue could be extended to determine the effects of ageing and disease on the arterial wall as a function of intraluminal pressure, given that changes in intraluminal pressure significantly affect the 3D microstructure of arterial walls (Walton et al., 2015).

## 5. Conclusions

FM-AFM is a useful tool for measure the mechanical properties of soft tissues such as the aorta and is a method that can be easily conducted using a conventional AFM by making use of ‘cantilever tuning’. We show that the technique can be used to probe age-related regional variations in the elastic and viscoelastic properties of ovine aorta. The FM-AFM data matches the trends in elastic behaviour we have previously reported with ultra-high frequency acoustic microscopy but provides new insight into viscoelastic changes in the aorta with age.

## Acknowledgments

We gratefully acknowledge funding from the Royal Society for the provision of an International Travel Grant for Collaboration (R112205) to RA, and Wellcome Trust Value in People Award to RA and MJS. MJS and BD gratefully acknowledge the support of the Medical Research Council (www.mrc.ac.uk: grant reference G1001398).

## References

- Akhtar, R., 2014. In vitro characterisation of arterial stiffening: From the macro- to the nano-scale. *Artery Research* 8, 1-8.
- Akhtar, R., Cruickshank, J.K., Zhao, X., Walton, L.A., Gardiner, N.J., Barrett, S.D., Graham, H.K., Derby, B., Sherratt, M.J., 2014. Localized micro- and nano-scale remodelling in the diabetic aorta. *Acta Biomater* 10, 4843-4851.
- Akhtar, R., Schwarzer, N., Sherratt, M.J., Watson, R.E., Graham, H.K., Trafford, A.W., Mummery, P.M., Derby, B., 2009. Nanoindentation of histological specimens: Mapping the elastic properties of soft tissues. *J Mater Res* 24, 638-646.
- Akhtar, R., Sherratt, M.J., Cruickshank, J.K., Derby, B., 2011. Characterizing the elastic properties of tissues. *Mater Today* 14, 96-105.
- Cerreta, A., Vobornik, D., Dietler, G., 2013. Fine DNA structure revealed by constant height frequency modulation AFM imaging. *European Polymer Journal* 49, 1916-1922.
- Dibb, K.M., Rueckschloss, U., Eisner, D.A., Isenberg, G., Trafford, A.W., 2004. Mechanisms underlying enhanced cardiac excitation contraction coupling observed in the senescent sheep myocardium. *J Mol Cell Cardiol* 37, 1171-1181.
- Gavara, N., Chadwick, R.S., 2010. Noncontact microrheology at acoustic frequencies using frequency-modulated atomic force microscopy. *Nat Methods* 7, 650-654.
- Gavara, N., Roca-Cusachs, P., Sunyer, R., Farré, R., Navajas, D., 2008. Mapping Cell-Matrix Stresses during Stretch Reveals Inelastic Reorganization of the Cytoskeleton. *Biophys J* 95, 464-471.
- Gosline, J., Lillie, M., Carrington, E., Guerette, P., Ortlepp, C., Savage, K., 2002. Elastic proteins: biological roles and mechanical properties. *Philos Trans R Soc Lond B Biol Sci* 357, 121-132.
- Graham, H.K., Akhtar, R., Kridiotis, C., Derby, B., Kundu, T., Trafford, A.W., Sherratt, M.J., 2011. Localised micro-mechanical stiffening in the ageing aorta. *Mech Ageing Dev* 132, 459-467.
- Grant, C.A., Twigg, P.C., 2013. Pseudostatic and dynamic nanomechanics of the tunica adventitia in elastic arteries using atomic force microscopy. *ACS Nano* 7, 456-464.
- Greenwald, S.E., 2007. Ageing of the conduit arteries. *J Pathol* 211, 157-172.
- Hemmasizadeh, A., Autieri, M., Darvish, K., 2012. Multilayer material properties of aorta determined from nanoindentation tests. *J Mech Behav Biomed Mater* 15, 199-207.
- Higgins, M.J., Riener, C.K., Uchihashi, T., Sader, J.E., McKendry, R., Jarvis, S.P., 2005. Frequency modulation atomic force microscopy: a dynamic measurement technique for biological systems. *Nanotechnology* 16, S85-S89.
- Holzappel, G.A., Gasser, T.C., Stadler, M., 2002. A structural model for the viscoelastic behavior of arterial walls: Continuum formulation and finite element analysis. *Eur J Mech a-Solid* 21, 441-463.
- Humphris, A.D.L., Tamayo, J., Miles, M.J., 2000. Active quality factor control in liquids for force spectroscopy. *Langmuir* 16, 7891-7894.
- Huynh, J., Nishimura, N., Rana, K., Peloquin, J.M., Califano, J.P., Montague, C.R., King, M.R., Schaffer, C.B., Reinhart-King, C.A., 2011. Age-Related Intimal Stiffening Enhances Endothelial Permeability and Leukocyte Transmigration. *Science translational medicine* 3, 112ra122-112ra122.

1 Kohn, J.C., Lampi, M.C., Reinhart-King, C.A., 2015. Age-related vascular stiffening: causes and  
2 consequences. *Frontiers in Genetics* 6, 112.  
3 Lin, D.C., Shreiber, D.I., Dimitriadis, E.K., Horkay, F., 2009. Spherical indentation of soft matter  
4 beyond the Hertzian regime: numerical and experimental validation of hyperelastic models.  
5 *Biomechanics and modeling in mechanobiology* 8, 345-358.  
6 Lopez-Andres, N., Rousseau, A., Akhtar, R., Calvier, L., Inigo, C., Labat, C., Zhao, X.G., Cruickshank, K.,  
7 Diez, J., Zannad, F., Lacolley, P., Rossignol, P., 2012. Cardiotrophin 1 Is Involved in Cardiac, Vascular,  
8 and Renal Fibrosis and Dysfunction. *Hypertension* 60, 563-+.  
9 Matsumoto, T., Goto, T., Furukawa, T., Sato, M., 2004. Residual stress and strain in the lamellar unit  
10 of the porcine aorta: experiment and analysis. *J Biomech* 37, 807-815.  
11 McKee, C.T., Last, J.A., Russell, P., Murphy, C.J., 2011. Indentation versus tensile measurements of  
12 Young's modulus for soft biological tissues. *Tissue Eng Part B Rev* 17, 155-164.  
13 O'Connell, M.K., Murthy, S., Phan, S., Xu, C., Buchanan, J., Spilker, R., Dalman, R.L., Zarins, C.K., Denk,  
14 W., Taylor, C.A., 2008. The three-dimensional micro- and nanostructure of the aortic medial lamellar  
15 unit measured using 3D confocal and electron microscopy imaging. *Matrix Biol* 27, 171-181.  
16 Petrie, R.J., Gavara, N., Chadwick, R.S., Yamada, K.M., 2012. Nonpolarized signaling reveals two  
17 distinct modes of 3D cell migration. *The Journal of Cell Biology* 197, 439-455.  
18 Silver, F.H., Horvath, I., Foran, D.J., 2001. Viscoelasticity of the vessel wall: the role of collagen and  
19 elastic fibers. *Crit Rev Biomed Eng* 29, 279-301.  
20 Walton, L.A., Bradley, R.S., Withers, P.J., Newton, V.L., Watson, R.E., Austin, C., Sherratt, M.J., 2015.  
21 Morphological Characterisation of Unstained and Intact Tissue Micro-architecture by X-ray  
22 Computed Micro- and Nano-Tomography. *Scientific reports* 5.  
23 Yin, F.C., Spurgeon, H.A., Kallman, C.H., 1983. Age-associated alterations in viscoelastic properties of  
24 canine aortic strips. *Circ Res* 53, 464-472.  
25 Zhao, X.G., Akhtar, R., Nijenhuis, N., Wilkinson, S.J., Murphy, L., Ballestrem, C., Sherratt, M.J.,  
26 Watson, R.E.B., Derby, B., 2012. Multi-Layer Phase Analysis: Quantifying the Elastic Properties of Soft  
27 Tissues and Live Cells with Ultra-High-Frequency Scanning Acoustic Microscopy. *Ieee T Ultrason Ferr*  
28 59, 610-620.  
29  
30  
31  
32  
33  
34  
35  
36  
37  
38  
39  
40  
41  
42  
43  
44  
45  
46  
47  
48  
49  
50  
51  
52  
53  
54  
55  
56  
57  
58  
59  
60  
61  
62  
63  
64  
65

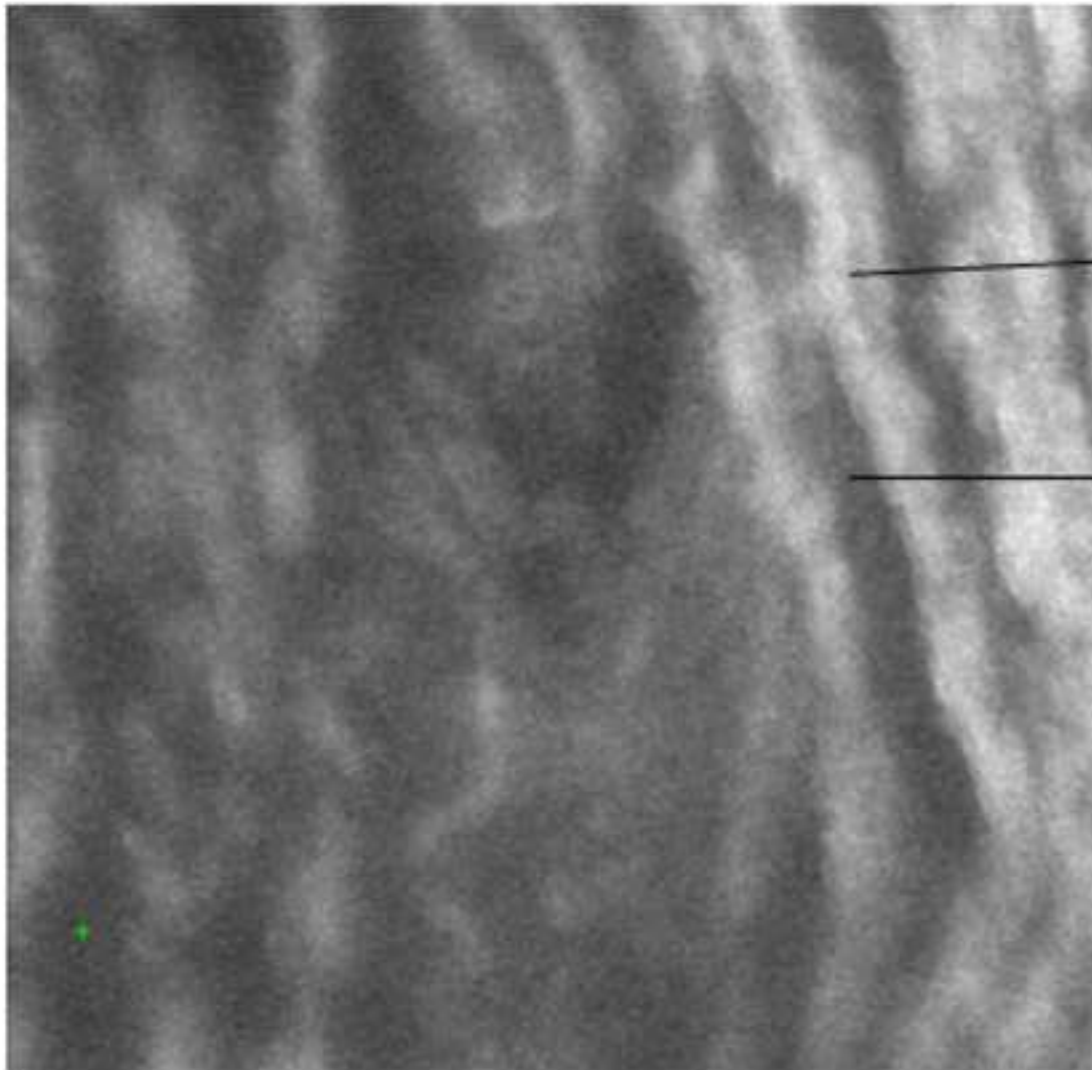
1  
2  
3 **Figure Captions**  
4

5 **Figure 1** Example optical image captured with the integrated microscope for localisation of  
6 lamellar and inter-lamellar regions of the medial layer. The size of the image 150x150  $\mu\text{m}$   
7 obtained with a 40X objective (880x880 pixels).  
8  
9

10  
11 **Figure 2** a) Individual and inter-animal variations in the mechanical properties of the medial  
12 layer. a) Elastic modulus of the medial layer for each animal in the young and old group b)  
13 Frequency distribution of the elastic modulus c) Frequency distribution of  $G'$  and d)  
14 Frequency distribution of  $G''$  in the young and old sheep aorta groups (n=55  
15 measurements/group with 11 measurements/animal).  
16  
17  
18  
19  
20

21 **Figure 3** Frequency distribution for the lamellar and inter-lamellar regions of the medial  
22 layer for a) Elastic modulus b)  $G'$  c)  $G''$  in the young and old sheep aorta groups (n=24  
23 measurements/group). The histogram distributions were found to be statistically significant  
24 in each group (Kruskal-Wallis ANOVA,  $P < 0.05$  for lamellar regions and  $P < 0.01$ ).  
25  
26  
27  
28  
29  
30  
31  
32  
33  
34  
35  
36  
37  
38  
39  
40  
41  
42  
43  
44  
45  
46  
47  
48  
49  
50  
51  
52  
53  
54  
55  
56  
57  
58  
59  
60  
61  
62  
63  
64  
65

**Figure 1**  
[Click here to download high resolution image](#)



Lamellar

Inter-Lamellar

Figure 2  
[Click here to download high resolution image](#)

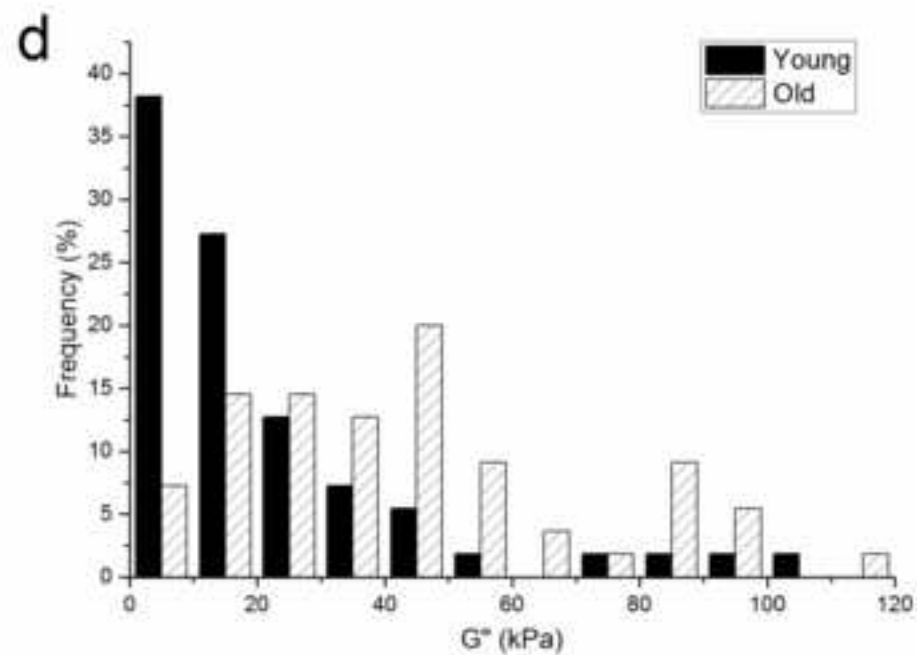
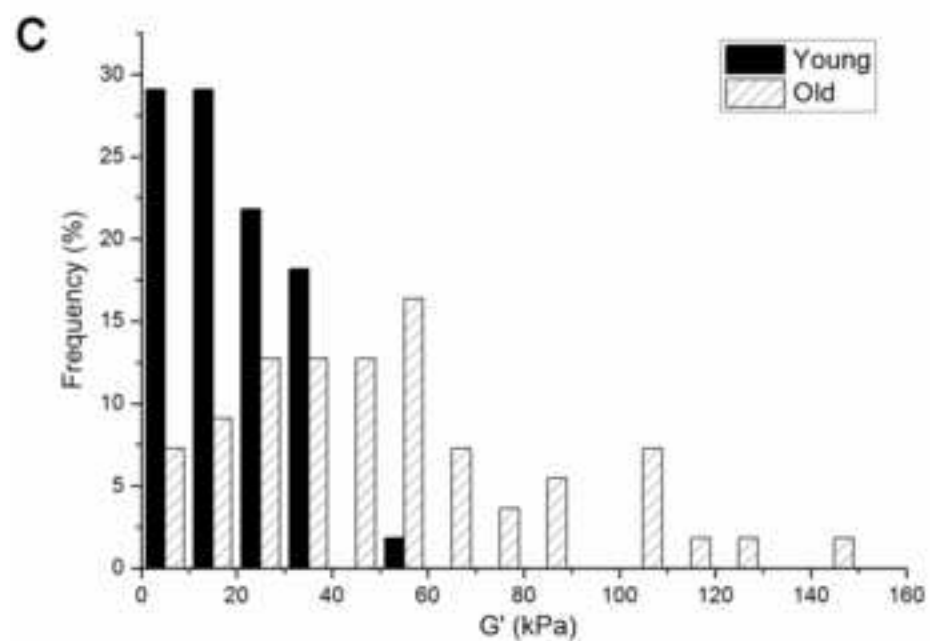
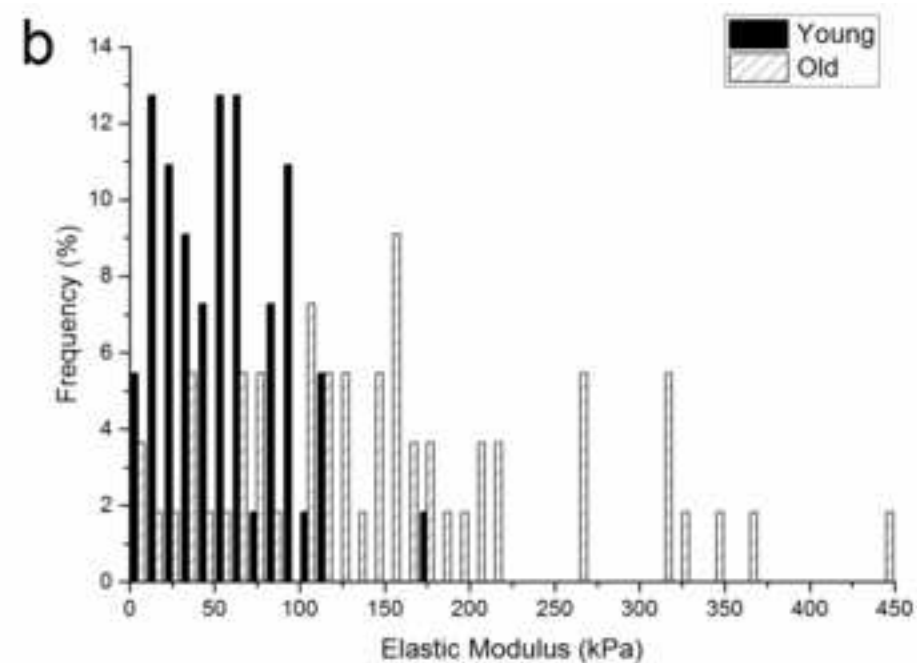
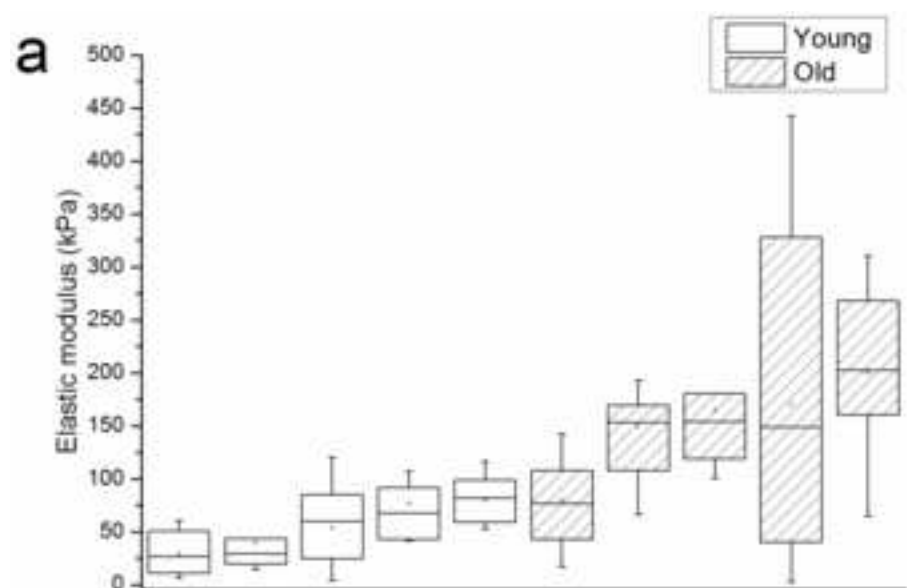
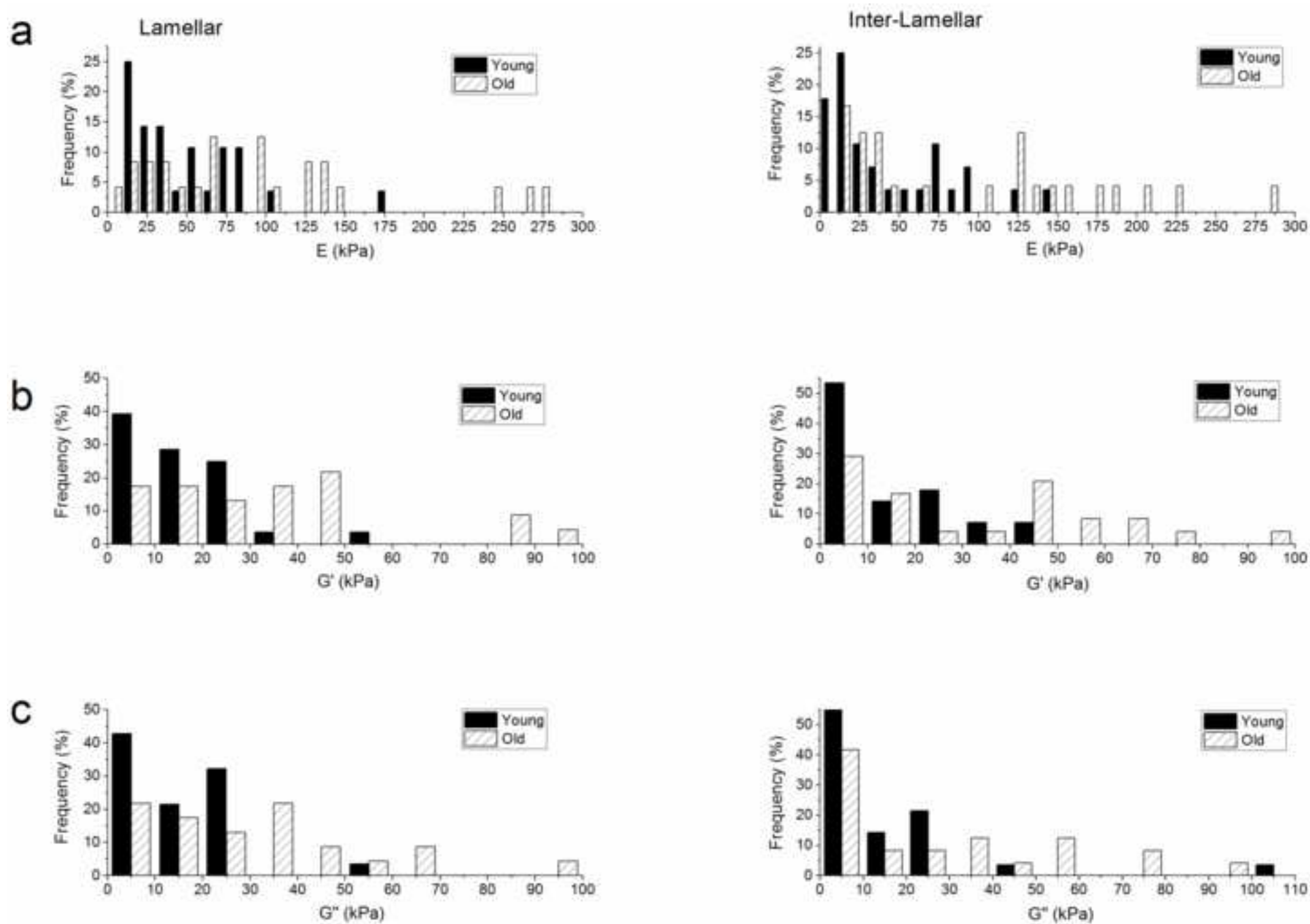


Figure 3  
[Click here to download high resolution image](#)



**Table 1 Mechanical properties determined for the young and old sheep aorta. Data is presented as geometric mean (geoSD).**

|           | Young       | Old          | P-Value  |
|-----------|-------------|--------------|----------|
| E (kPa)   | 42.9 (2.26) | 113.9 (2.57) | P<0.0001 |
| G' (kPa)  | 14.3 (2.26) | 38.0 (2.57)  | P<0.0001 |
| G'' (kPa) | 14.5 (2.56) | 32.8 (2.52)  | P<0.0001 |

**Table 2 Mean values for the mechanical properties determined for the lamellar and inter-lamellar regions of the medial for the young and old sheep aorta. Data is presented as geometric mean (geoSD).**

|              | Lamellar<br>(Young) | Lamellar<br>(Old) | P-Value<br>(Lamellar) | Inter-<br>lamellar<br>(Young) | Inter-lamellar<br>(Old) | P-Value<br>(Inter-<br>lamellar) |
|--------------|---------------------|-------------------|-----------------------|-------------------------------|-------------------------|---------------------------------|
| E<br>(kPa)   | 36.4 (2.22)         | 63.5 (2.95)       | P<0.05                | 25.3 (3.39)                   | 63.7 (2.76)             | P<0.01                          |
| G'<br>(kPa)  | 12.1 (2.22)         | 24.3 (2.37)       | P<0.05                | 8.42 (3.39)                   | 21.2 (2.76)             | P<0.01                          |
| G''<br>(kPa) | 10.6 (2.77)         | 20.1 (2.67)       | P<0.05                | 6.73 (3.98)                   | 17.5 (3.02)             | P<0.01                          |